Chemical Engineering Journal 306 (2016) 233–241

Contents lists available at ScienceDirect

Chemical Engineering Journal

journal homepage: www.elsevier.com/locate/cej

Simplified model for hydrogenotrophic denitrification in an unsaturated-flow pressurized reactor

Razi Epsztein *, Michael Beliavski, Sheldon Tarre, Michal Green

Faculty of Civil and Environmental Engineering, Technion – Israel Institute of Technology, Haifa 32000, Israel

HIGHLIGHTS

- A model for H_2-based denitrifier unsaturated-flow pressurized reactor is presented.
- The rate constant and k_La were determined for different recirculation flow rates.
- A correction factor for the rate constant was successfully developed.
- High correlation between model and experimental results was achieved.
- Max. denitrification rate of 7.5 gNO_3^--N/($L_{reactor}$·d) was predicted by the model.

GRAPHICAL ABSTRACT

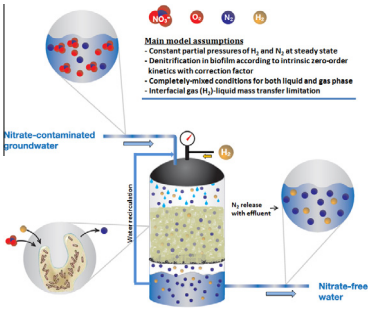

ARTICLE INFO

Article history:
Received 26 April 2016
Received in revised form 14 June 2016
Accepted 5 July 2016
Available online 13 July 2016

Keywords:
Biodegradation
Bioreactor
Hydrogenotrophic denitrification
Modeling
Trickle bed
Water recirculation

ABSTRACT

A novel unsaturated-flow pressurized reactor (UFPR) for hydrogenotrophic denitrification was recently developed. The reactor is characterized by safe and economic operation since gas purging intrinsic to conventional H_2-based systems is not required and H_2 loss is limited only to the dissolved H_2 in the effluent. Additionally, high denitrification rates are achieved by high water recirculation over plastic carriers with high surface area.

This paper focuses on mathematical modeling of the novel reactor, based on its unique and specific characteristics. The continuously stirred hydraulic regime formed due to the relatively high recirculation flow rate required for efficient media wetting and the homogeneous gas phase in the closed reactor headspace, simplified the model design for the UFPR. The reaction rate constant and the overall volumetric gas (H_2)-liquid mass transfer coefficient (k_La) were determined for different recirculation flow rates at steady state. A rate constant correction factor β was developed to compensate for pH changes within the biofilm, deviation from intrinsic zero-order degradation kinetics and non-homogeneity of the biofilm. Model validation tests showed a high correlation between experimental and model results for various combinations of operational parameters. Results from the model showed that high denitrification rates of up to 7.5 g NO_3^--N/($L_{reactor}$·d) together with H_2 utilization efficiencies above 90% can be achieved by the UFPR.

© 2016 Elsevier B.V. All rights reserved.

1. Introduction

Hydrogen-based denitrification systems for treating nitrate-contaminated groundwater have gained a lot of attention in recent years. The clear advantages of hydrogenotrophic systems over reactors using traditional organic compounds as electron donors for reducing NO_3^- have been extensively discussed in previous works and include mainly low biomass yield, minimization of reactor clogging and reduction of post-treatment costs. However, safety concerns, poor utilization of H_2 gas and low denitrification rates are the main drawbacks still limiting the implementation of this method in full scale [1].

* Corresponding author.
E-mail address: epsztein@tx.technion.ac.il (R. Epsztein).

http://dx.doi.org/10.1016/j.cej.2016.07.020
1385-8947/© 2016 Elsevier B.V. All rights reserved.

Nomenclature

A	total active surface area for bacterial growth [m^2/m^3]
β_H	empirical correction factor for K_H
β_N	empirical correction factor for K_N
C_{H_2}	Henry's constant for H_2 gas [mg/(L·bar)]
C_{N_2}	Henry's constant for N_2 gas [mg/(L·bar)]
$D_{f,H}$	diffusion coefficient of H_2 in the biofilm [m^2/d]
$D_{f,N}$	diffusion coefficient of NO_3^- in the biofilm [m^2/d]
H^*	equilibrium concentration of dissolved H_2 [mg/L]
H_{av}	average concentration of dissolved H_2 along the filter [mg/L]
H_e	effluent concentration of dissolved H_2 [mg/L]
H_i	inlet concentration of dissolved H_2 [mg/L]
K_H	half-order coefficient for H_2 degradation [$(mg/L)^{0.5}$/d]
K_N	half-order coefficient for NO_3^--N degradation [$(mg/L)^{0.5}$/d]
$k_{0f,H}$	degradation rate of H_2 in the biofilm [g/($L_{biofilm}$·d)]
$k_{0f,N}$	degradation rate of NO_3^--N in the biofilm [g/($L_{biofilm}$·d)]
k_La	overall volumetric gas-liquid mass transfer coefficient of H_2 [1/d]
N_{av}	average concentration of NO_3^--N along the filter [mg/L]
N_e	effluent concentration of NO_3^--N [mg/L]
N_i	inlet concentration of NO_3^--N [mg/L]
$N_{2,T}$	total dissolved N_2 concentration [mg/L]
$N_{2,atm}$	dissolved N_2 concentration originated from atmospheric N_2 gas [mg/L]
$N_{2,denit}$	dissolved N_2 concentration originated from denitrification [mg/L]
P_{H_2}	partial pressure of H_2 gas in the reactor [bar]
P_{N_2}	partial pressure of N_2 gas in the reactor [bar]
P_T	total pressure in the reactor [bar]
$q_{max,N}$	maximal specific degradation rate of NO_3^--N [g/(gVSS·d)]
Q	volumetric flow rate [mL/min]
Q_R	recirculation flow rate [mL/min]
r_H	overall degradation rate of H_2 [g/($L_{reactor}$·d)]
r_N	overall degradation rate of NO_3^--N [g/($L_{reactor}$·d)]
t	time component [d]
V	reactor volume [L]
υ	stoichiometric mass ratio [g H_2/g NO_3^--N]
X_f	biofilm density [gVSS/mL]

A novel unsaturated-flow pressurized reactor (UFPR) for hydrogenotrophic denitrification of groundwater operating at high denitrification rates together with minimal hydrogen loss and low risk was presented and described in an earlier publication [2]. The main novelty of this reactor is the operation under a pressurized closed headspace without any gas discharge. The common concern of N_2 gas build-up in a pressurized denitrifying system is addressed by the idea that in continuous operation a gas-liquid equilibrium is achieved according to Henry's law and the effluent water carries excess N_2 gas out of the reactor. Since N_2 reaches equilibrium and is not accumulated over time, there is no need for gas discharge and H_2 loss to atmosphere is limited only to the dissolved H_2 in the effluent. The operation under low-pressurized headspace consisting uniquely of H_2 and N_2 gases prevents hazardous H_2—O_2 contact and minimizes the risk of explosion in case of failure.

On top of the inherent advantages of safety and economics, the UFPR was designed to ensure high denitrification rates in comparison to existing hydrogenotrophic systems. The reactor is operated under an unsaturated-flow regime as a trickling filter where water is recirculated over plastic biofilm carriers with high surface area. The high surface area of the plastic carriers serves as a platform for both bacterial growth and gas (H_2)-liquid mass transfer, thus enabling high denitrification rates. Utilization of plastic carriers with very high surface area in unsaturated-flow reactors is susceptible to reactor clogging and is more commonly implemented in autotrophic trickling filters with low cell yield as in nitrification or the UFPR. In these systems very often a relatively high recirculation flow rate is applied in order to achieve full media wetting [3]. The recirculation ratio (Q_R/Q) applied in the UFPR varies between 3 and 18, which is about one order of magnitude higher than the recirculation ratio in traditional trickling filters [4]. This high recirculation ratio, together with the assumption of a well-mixed and homogeneous gas phase in the closed headspace, differentiates the UFPR from traditional trickling filters; especially in terms of reactor hydraulics.

Trickling filter models attempt to take into account various processes affecting the contaminant degradation such as gas flow, phase transfer, diffusion within the biofilm, biological growth and structural changes of the biofilm. Due to the problematic characterization of the unsaturated flow through the carriers and its poorly understood mechanics, most of the models and design approaches of trickling filters are empirical and therefore case specific [4–6]. The main objective of the current study is to develop a simplified and easy-to-use model for basic design and performance forecast of the UFPR, based on its unique operational conditions of unsaturated flow with high recirculation flow rate and operation in a closed headspace. Special focus is given to the effect of recirculation flow rate on reactor performance.

2. Considerations and guidelines for model design

Based on model objectives, the following assumptions were taken for model design: (1) steady-state conditions exist for all phases (gas, liquid and biofilm); (2) the biofilm is planar, one dimensional and completely homogeneous with uniform density X_f; (3) the diffusion layer near the biofilm surface is neglected, i.e., the substrate concentrations on the biofilm surface equals the bulk concentration; (4) mathematical models of hydrogenotrophic denitrification are generally described by zero-order kinetics when substrate concentrations are much higher than the half-saturation constants (i.e. $S_{NO_3} \gg K_{NO_3}$ and $S_{H_2} \gg K_{H_2}$) [7–9]. Therefore, a NO_3^--N reduction based on zero-order kinetics in the biofilm is assumed. Importantly, application of a zero-order kinetic model in biofilm reactors should be considered more carefully due to the gradual decrease of substrate concentration with increasing depth of the biofilm, as was also discussed by Atkinson et al. [10]. Moreover, in the case of denitrification, the pH gradient formed within the biofilm might also affect the maximal specific degradation rate q_{max} along the biofilm. Accordingly, a correction factor is added to the standard zero-order-based reaction rate constant for degradation in the biofilm to take into account these factors as will be explained later; (5) due to the high diffusivity of H_2 in the gas phase of the UFPR, the rate limiting step for H_2 transfer is the interfacial gas-liquid transfer; (6) in the UFPR a high recirculation ratio is applied so that the entire trickling filter may be considered as a single CSBR (continuously stirred biofilm reactor) unit with a uniform concentration of NO_3^--N throughout the reactor. This assumption can be applied also for the dissolved H_2 concentration due to the following reason: since the reactor headspace is sealed (i.e. pressurized), no natural gas convection (i.e. air draft) occurs as in traditional trickling filters. Therefore, assuming good mixing of the gas phase by molecular diffusion, any gradient of

H_2 concentration in the gas phase along the filter can be neglected and the driving force for gas-liquid transfer (i.e. the term (C^*-C) in Eq. (5) below) should have approximately the same value at any position in the reactor. Nevertheless, a minor gradient of the bulk concentration (i.e. S^b in Eq. (1) below) for both substrates is expected along the filter axis even at high recirculation ratios, i.e., the effluent concentration in the reactor's bottom S_e is slightly different than the concentration in the top part of the reactor where recirculated water is mixed with the inlet flow. Therefore, an average bulk substrate concentration along the filter axis, different than the effluent concentration S_e, is taken for model design.

Utilizing assumptions (1) through (4), the expression for penetration depth of the rate-limiting substrate to the biofilm can be described by Eq. (1) [11].

$$L_{pen} = \sqrt{2S^b D_f / k_{0f}} \tag{1}$$

where L_{pen} is the penetration depth of the rate-limiting substrate; S^b is the bulk concentration of the rate-limiting substrate; D_f is the diffusivity of the rate-limiting substrate in the biofilm and k_{0f} is the degradation rate of the rate-limiting substrate within the biofilm and expressed by Eq. (2).

$$k_{0f} = q_{\max} X_f \tag{2}$$

where $q_{\max}$ is the maximal specific degradation rate of the rate limiting substrate and X_f is the biofilm density.

In an ideal CSBR (see assumption (6) above), the penetration depth of the rate-limiting substrate is uniform throughout the reactor, so the overall rate of substrate degradation in the reactor can be evaluated by Eq. (3).

$$r = k_{0f}\ A\ L_{pen} \tag{3}$$

where r is the overall rate of substrate degradation in the reactor and A is the total active surface area for bacterial growth. The combination of Eqs. (1) and (3) gives Eq. (4).

$$r = A\sqrt{2S^b D_f k_{0f}} \tag{4}$$

Following assumptions (5) and (6), the volumetric gas-liquid transfer rate through the gas-liquid interface can be described by Eq. (5) [12].

$$dC/dt = k_L\alpha(C^* - C) \tag{5}$$

where C is the concentration in liquid; C^* is the equilibrium concentration in the liquid according to Henry's law and k_La is the overall volumetric gas-liquid mass transfer coefficient. In the k_La expression, k_L equals to (D/δ) and a equals to (A/V), where D is the diffusivity in the interfacial liquid film; δ is the width of the interfacial liquid film; A is the interfacial surface area and V is the representative volume, usually taken as the liquid volume or the overall volume of the system. The k_La is highly affected by temperature, flow conditions and the interfacial gas-liquid surface area, and can be calculated mechanistically [13] or estimated empirically from mass balance equations [14]. In the UFPR, k_La can be evaluated empirically by analytical solution of the mass balance equations as will be shown later.

Eqs. (6) and (7) describe the general mass balances in the reactor for NO_3^--N and dissolved H_2, respectively.

$$V(dN_e/dt) = Q(N_i - N_e) - r_N V \tag{6}$$

$$V(dH_e/dt) = k_L\alpha(H^* - H_{av})V + Q(H_i - H_e) - r_H V \tag{7}$$

where V is the reactor volume; N_e and H_e are the concentration of NO_3^--N and dissolved H_2 in the effluent, respectively; k_La is the overall volumetric gas-liquid mass transfer coefficient of H_2; H_{av} is the average concentration of dissolved H_2 along the filter; t is the time component; Q is the volumetric flow rate; N_i and H_i are the concentration of NO_3^--N and dissolved H_2 in the influent, respectively; H^* is the equilibrium concentration of dissolved H_2 and r_N and r_H are the overall degradation rates of NO_3^--N and dissolved H_2, respectively.

Following assumption (1) above and assuming that the concentration of dissolved H_2 in the influent is close to zero ($H_i \approx 0$), at steady-state conditions Eqs. (6) and (7) can be simplified to form Eqs. (8) and (9), respectively.

$$0 = Q(N_i - N_e) - r_N V \tag{8}$$

$$0 = k_L\alpha(H^* - H_{av})V - QH_e - r_H V \tag{9}$$

H^* is calculated according to Henry's law by Eq. (10).

$$H^* = P_{H_2} C_{H_2} \tag{10}$$

where C_{H_2} is Henry's constant for H_2 in units of mg/(L·bar) and P_{H_2} is the partial pressure of H_2 gas in the reactor calculated by Eq. (11) according to the concept developed [2].

$$P_{H_2} = P_T - P_{N_2} \tag{11}$$

where P_T is the total pressure (i.e., pressure of H_2 and N_2 gases) in the reactor and P_{N_2} is the partial pressure of N_2 gas in the reactor calculated by Eq. (12) according to Henry's law.

$$P_{N_2} = N_{2,T}/C_{N_2} \tag{12}$$

where C_{N_2} is Henry's constant for N_2 in units of mg/(L·bar) and $N_{2,T}$ is the total dissolved N_2 concentration calculated by Eq. (13).

$$N_{2,T} = N_{2,atm} + N_{2,denit} \tag{13}$$

where $N_{2,atm}$ is the dissolved N_2 concentration originated from atmospheric N_2 gas (assumed to be constant at stable outdoor temperature) and $N_{2,denit}$ is the dissolved N_2 concentration originated from denitrification and calculated by Eq. (14).

$$N_{2,denit} = 0.96\ (N_i - N_e) \tag{14}$$

where 0.96 is the fraction of NO_3^--N converted to N_2 (catabolism) according to the hydrogenotrophic dentirification metabolic stoichiometry equation suggest by McCarty [15].

Eqs. (15) and (16) describe r_N and r_H in Eqs. (8) and (9) for conditions of NO_3^--N and H_2 limitation, respectively, according to Eq. (4).

$$NO_3^- - N \text{ limitation}: r_N = A\sqrt{2D_{f,N}k_{0f,N}N_{av}}; \quad r_H = \upsilon r_N \tag{15}$$

$$H_2 \text{ limitation}: r_N = \left(\frac{1}{\upsilon}\right) r_H; \quad r_H = A\sqrt{2D_{f,H}k_{0f,H}H_{av}} \tag{16}$$

where the terms $A\sqrt{2D_{f,N}k_{0f,N}}$ and $A\sqrt{2D_{f,H}k_{0f,H}}$, the half-order coefficients for NO_3^--N and H_2, respectively, will be referred to as K_N and K_H, respectively; $D_{f,N}$ and $D_{f,H}$ are the diffusivities of NO_3^- and H_2 in the biofilm, respectively; $k_{0f,N}$ and $k_{0f,H}$ are the intrinsic maximal degradation rates ($q_{\max}X_f$) of NO_3^--N and H_2 in the biofilm, respectively; A is the total active surface area for bacterial growth; υ is the stoichiometric mass ratio {H_2:NO_3^--N}; and N_{av} and H_{av} are the average bulk concentrations of NO_3^--N and dissolved H_2 along the filter, respectively, calculated as a simple mean of the concentration in the upper part of the column (i.e. merge of recirculation flow and inflow) and in the effluent (Eq. (17a) and (17b)).

$$N_{av} = \frac{\frac{N_i Q + N_e Q_R}{Q + Q_R} + N_e}{2}; \tag{17a}$$

$$H_{av} = \frac{\frac{H_i Q + H_e Q_R}{Q + Q_R} + H_e}{2} \tag{17b}$$

where Q_R is the recirculation flow rate.

Interestingly, preliminary observations showed that the half-order coefficients K_N and K_H vary with different average bulk concentration of the rate-limiting substrate (i.e. N_{av} or H_{av}, respectively). Therefore, new terms β_N and β_H were incorporated to correct K_N and K_H, respectively, for a specific average bulk concentration of the rate-limiting substrate. The correction factors β_N and β_H are required in order to take into account the influence of pH increase in the biofilm on q_{max}, deviation from zero-order degradation kinetics within the biofilm due to low substrate concentrations and non-homogeneity of the biofilm. These three mechanisms are assumed to depend on the average bulk concentration of the rate-limiting substrate, as discussed in Section 4.2.

Following the above consideration, the terms r_N and r_H in Eqs. (15) and (16) can be modified to form Eqs. (15′) and (16′), respectively.

$$NO_3^- - \text{N limitation}: \; r'_N = \beta_N A\sqrt{2D_{f,N}k_{0f,N}N_{av}}; \; r'_H = \upsilon r_N \tag{15'}$$

$$H_2 \text{ limitation}: \; r'_N = \left(\frac{1}{\upsilon}\right) r_H; \; r'_H = \beta_H A\sqrt{2D_{f,H}k_{0f,H}H_{av}} \tag{16'}$$

where β_N and β_H are the correction factors for the half-order coefficients K_N and K_H, respectively, and defined by Eq. (18a) and (18b).

$$\beta_N = f_1(N_{av}); \tag{18a}$$

$$\beta_H = f_2(H_{av}) \tag{18b}$$

where f_1 and f_2 are functions describing β_N and β_H, respectively.

k_La in Eq. (9) and A in Eqs. (15) and (16) are assumed to depend on the total flow rate over the media, i.e. the sum of recirculation flow rate and the volumetric flow rate (Eqs. (19) and (20)).

$$k_La = f_3(Q_R + Q) \tag{19}$$

$$A = f_4(Q_R + Q) \tag{20}$$

where f_3 and f_4 are functions describing k_La and A, respectively.

A detailed list summarizing the main model variables is shown in Table 1.

In Table 1, input variables are defined as independent variables controlled directly by the operator or dictated by the local constraints. Intermediate variables are defined as variables that depend uniquely on specific input variables and are not controlled directly by the operator. Output variables depend on a complex ensemble of all input and intermediate variables. The empirical correction factors β_N and β_H are exceptional intermediate variables, depending on a preliminary assessment of the average bulk substrate concentration of the rate-limiting substrate (i.e. N_{av} or H_{av}). Other important parameters can be derived from the output variables such as denitrification rate and H_2 utilization efficiency.

Since input variables are given, model solution (i.e. calculation of all output variables) can be accomplished after finding the functions describing the intermediate variables (see Eqs. (18a), (18b), (19) and (20)), which link the input and the output variables. Therefore, evaluation of the intermediate variables for different sets of conditions is the main stage in model development. Detailed explanations and test protocols of methods to assess the intermediate variables are given in the next section.

3. Materials and methods

3.1. Experimental setup

The unsaturated-flow pressurized reactor (UFPR) used for all continuous tests is shown in Fig. 1. A detailed description of the system and reactor start-up was given in an earlier publication [2]. Briefly, it comprised of a clear PVC cylindrical reactor 71 cm in height and 10.5 cm in diameter divided into two unequal parts. The top part of the reactor (height 51 cm) contained plastic biofilm carriers (total surface of 900 m^2/m^3, Aqwise) and was separated by a metal screen from the bottom part (height 20 cm) of the reactor where recirculating water collected. The reactor was connected to a gas supply (H_2 cylinder with pressure regulator), feed pump (Diaphragm pump model 7090-42, Cole-Palmer), recirculation pump (FL-2403, ProPumps) and pH controlling unit (standard pH electrode, pH controller – pH190, Alpha; hydrochloric acid tank and acid pump – gamma/L, ProMinent).

The feed solution for all experiments was tap water mixed with concentrated stock solutions of $NaNO_3$ and KH_2PO_4. The specific operational conditions used for each test are elaborated in the test protocols section. Water temperature was maintained constant at 27.5 ± 1 °C. Bulk pH was kept at 7 ± 0.1 by dosing hydrochloric acid. The relatively low pH was aimed to prevent an extreme pH increase within the biofilm, which leads to NO_2^--N accumulation [7,16]. Influent and effluent water were collected for further analyses.

For all continuous experiments, the system was first operated to steady state with the highest Q_R (i.e. 8000 mL/min), high average NO_3^--N concentration above 20 mg/L (i.e. N_{av} > 20 mg/L) and high H_2 pressure of 3 bars, achieved by continuous gas flushing of the reactor's headspace with H_2 gas under pressure of 3 bars. The volumetric flow rate was 450 mL/min and N_{av} was controlled by adjusting the inlet NO_3^--N concentration (i.e. N_i). For the current research purposes, steady state was defined as an operational state presenting constant denitrification rate during extended operation.

Table 1
Detailed list of the main model variables.

Variable	Symbol	Type of variable	Dependency
Volumetric flow rate	Q	Input	Operator
NO_3^--N inlet concentration	N_i	Input	Local constraints
Total pressure	P_T	Input	Operator
Reactor volume	V	Input	Operator
Recirculation flow rate	Q_R	Input	Operator
Total flow rate	$Q_R + Q$	Input	Operator
Overall volumetric gas (H_2)-liquid mass transfer coefficient	k_La	Intermediate	Q_R and Q
Half-order coefficient	K_N, K_H	Intermediate	Q_R and Q
Empirical correction factors for K_N and K_H	β_N, β_H	Intermediate	See explanation in body text below
NO_3^--N effluent concentration	N_e	Output	Input and intermediate variables
Dissolved H_2 effluent concentration	H_e	Output	Input and intermediate variables
Equilibrium concentration of dissolved H_2	H^*	Output	Input and intermediate variables
Partial pressure of H_2	P_{H_2}	Output	Input and intermediate variables
Partial pressure of N_2	P_{N_2}	Output	Input and intermediate variables

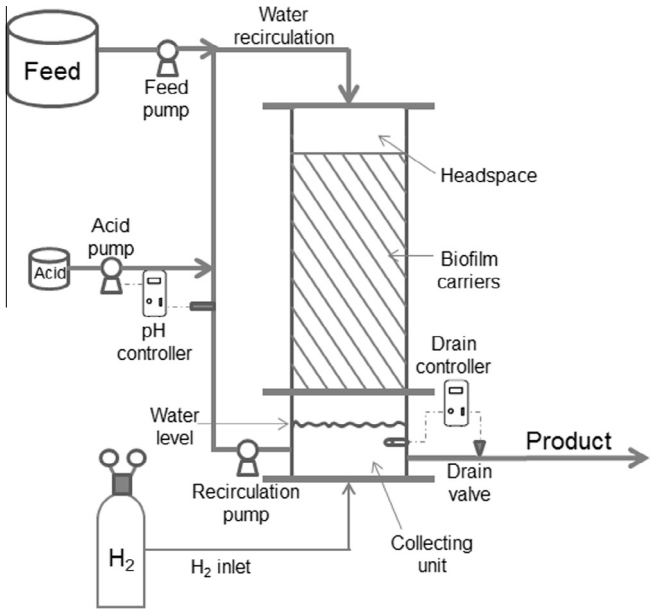

Fig. 1. Schematic diagram of the UFPR system.

All test protocols described in Section 3.4 were conducted after reaching steady state.

3.2. Preliminary batch experiment to determine the maximal specific degradation rate of NO_3^--N

The intrinsic maximal specific degradation rate of NO_3^--N, $q_{max,N}$, was found in a separate batch experiment with suspended growth medium at similar conditions as in the bulk liquid in the biofilm experiments (i.e. pH 7 and temperature of 27.5 °C). A 4.5 L mixed liquor volatile suspended solid (MLVSS) solution with biomass taken from the biofilm reactor was mixed with 2 L of tap water together with 3.7 g $NaNO_3$, 6 g $NaHCO_3$ and 0.3 g KH_2PO_4. A constant H_2 pressure of 2 bars was maintained during the experiment by continuous H_2 sparging. Nitrate-N concentration was measured over time and denitrification rate was calculated. Following measurement of the volatile suspended solids (VSS) concentration, $q_{max,N}$ was calculated using the Lineweaver-Burk plot method. The VSS concentration was measured according to Standard Methods (Method 2540).

3.3. Analytical methods

Nitrate was determined using a Metrohm 761 ion chromatograph (IC) equipped with a 150 mm Metrosep A Supp 5 column with column guard and suppressor using a CO_3^{-2}/HCO_3^- eluent. Nitrite-N and alkalinity were measured according to Standard Methods (Method 4500 and Method 2320, respectively).

Biofilm density X_f was measured by the following procedure: (1) biofilm originating from the experimental system was separated from the plastic carriers in tap water to create MLVSS solution; (2) a 25 mL of the MLVSS solution was allowed to settle in a 50 mL measuring cup; (2) after settling, the volumes of clear water phase and settled biomass phase were recorded; (3) the total volume was filtered and the biomass volume was calculated by subtracting the filtered water volume from the total tested volume (i.e. 25 mL); (4) VSS weight was measured; (5) biofilm density was calculated by dividing the VSS weight by the biomass volume.

3.4. Test protocols for assessment of model's intermediate variables

3.4.1. Assessment of the half-order coefficients K_N and K_H for different recirculation flow rates

In this experiment, H_2 was given in excess by continuous flushing of the reactor's headspace with H_2 gas under pressure of 3 bars. The average NO_3^--N concentration N_{av} was kept constant at 5 mg/L by adjusting the inlet NO_3^--N concentration N_i in the range of 20–40 mg/L. With NO_3^--N as the rate limiting substrate, Eq. (15) could be used and K_N and K_H were assessed for different Q_R values in the range of 1250–8000 mL/min. For each recirculation flow rate applied, N_i and N_e were measured, the denitrification rate r_N was calculated by Eq. (8) and K_N was calculated by Eq. (15). Finally, a mathematical expression for K_N as a function of the total flow rate (i.e. $Q_R + Q$) at $N_{av} = 5$ mg/L was derived in MS Excel and the corresponding expression for K_H was also determined as explained in Section 4.1.

3.4.2. Assessment of the correction factors β_N and β_H for K_N and K_H

For assessing β_N and β_H, H_2 was given in excess as described in Section 3.4.1. The recirculation flow rate Q_R was kept constant on 8000 mL/min and β_N and β_H were assessed for different N_{av} concentrations in the range of 0–20 mg/L by adjusting the N_i in the range of 10–75 mg/L. For each value of N_{av} tested, N_i and N_e were measured, the denitrification rate r_N was calculated by Eq. (8), the product $K_N\beta_N$ was calculated by Eq. (15′) and divided by the reference K_N calculated in Section 3.4.1 (i.e. K_N at $N_{av} = 5$ mg/L and $Q = 8000$ mL/min) to find β_N for the specific N_{av} value. Finally, a mathematical expression for β_N as a function of N_{av} was derived in MS Excel and the corresponding expression for β_H was also determined as explained in Section 4.2.

3.4.3. Assessment of the overall volumetric gas (H_2)-liquid mass transfer coefficient k_La for different recirculation flow rates

For assessing k_La values by Eq. (9), H_{av} values are initially had to be calculated by Eq. (16′). In order to use Eq. (16′), H_2 was set to be limiting by continuous flushing of the reactor's headspace with H_2 gas under a lower pressure of 1.5 bars and keeping the N_{av} values above 36 mg/L by applying a constant N_i of 65 mg/L. The k_La values were assessed for different Q_R values in the range of 1250–8000 mL/min. For each Q_R applied, the following procedure was performed: (1) N_i and N_e were measured; (2) the denitrification rate r_N was calculated by Eq. (8) and converted to H_2 degradation rate r_H by the stoichiometric mass ratio υ; (3) an initial assessment of H_{av} was done by Eq. (16) using the reference value of K_H calculated in Section 3.4.1; (4) the corresponding β_H for the initial H_{av} assessed was calculated by the expression derived in Section 3.4.2; (5) a corrected H_{av} value was calculated by Eq. (16′) using the corresponding β_H found; (6) effluent H_2 concentration (i.e. H_e) was calculated by Eq. (17b); (7) the overall volumetric gas-liquid mass transfer coefficient k_La was calculated analytically by Eq. (9) using the corresponding H^* for H_2 pressure of 1.5 bar according to Henry's law (i.e. $H^* \approx 2.3$ mg/L). Following these 7 steps for all values of Q_R tested, a mathematical expression for k_La as a function of the total flow rate was derived in MS Excel.

3.5. Model utilization

Two important points should be noted regarding model utilization: (1) Since the correction factors β_N and β_H depend on the average concentration of the rate-limiting substrate (i.e. N_{av} or H_{av}, which are output variables and not known at the beginning), a calculation of a preliminary set of output variables using Eqs. (15) or (16) is performed. The preliminary N_{av} and H_{av} calculated are then served to assess the corresponding values of β_N and β_H, respectively, according to the procedure described in Section 3.4.2.

Afterwards, a new set of output variables is calculated with β_N and β_H found. Theoretically, this procedure should be repeated to increase the model's accuracy. However, a single iteration gave satisfactory results in most cases. (2) Since the choice between Eq. (15) or (16) depends on which substrate is limiting (determined only after knowing the output variables N_{av} and H_{av}), both Eqs. (15) and (16) are initially used and the results are compared. The choice of the right equation to be carried forward during model use is tested in terms of substrate limitation by Eq. (21).

$$H_{av}/N_{av} = \upsilon \times (D_{f,N}/D_{f,H}) = 0.129\ gH_2/gNO_3^-N \quad (21)$$

Eq. (21) is a derivative of the equalization of Eq. (1) for N_{av} and H_{av}. The following values were taken for calculations: $\upsilon = 0.429$ g H_2/g NO_3^--N [15], $D_{f,N} = 8.15 \times 10^{-10}$ m^2/sec and $D_{f,H} = 2.7 \times 10^{-9}$ m^2/sec [17].

4. Results and discussion

4.1. Assessment of the half-order coefficients K_N and K_H for different recirculation flow rates

The first set of continuous experiments (see Section 3.4.1) with NO_3^--N as the rate limiting substrate was performed in order to assess K_N values ($K_N = A\sqrt{2D_{f,N}k_{0f,N}}$) at constant N_{av} concentration of 5 mg NO_3^--N/L for different recirculation flow rates (Q_R) by Eq. (15). The results for K_N at N_{av} = 5 as a function of the total flow rate are shown in Fig. 2.

As expected, K_N values (with the corresponding denitrification rates) increased significantly with higher recirculation flow rates due to the increase in media wetting which results in higher surface area of active biofilm (i.e. A in the expression of K_N above) exposed to both NO_3^--N and H_2 as discussed previously [2]. As mentioned above, the relatively high recirculation flow rate required to achieve full media wetting is mainly due to the high specific surface area of the carriers. High hydraulic loading rates were specifically reported for nitrifying trickling filters in recirculating aquaculture [3]. At $Q_R + Q \approx 8000$ mL/min, media wetting approached a maximal level. Further increase of Q_R was not possible due to technical issues. A trend line with R-squared coefficient value of 0.9995 was determined (Eq. (22)).

$$K_N = -3 \times 10^{-5}(Q_R + Q)^2 + 0.487(Q_R + Q) + 11.5 \quad (22)$$

The corresponding H_{av} concentration with the same penetration depth as 5 mg NO_3^--N/L was estimated by Eq. (21) to be 0.65 mg/L. A mathematical expression for K_H as a function of the total flow rate at H_{av} = 0.65 mg/L was derived by Eq. (23) and presented in Eq. (24).

$$K_H = K_N\sqrt{\upsilon \times (D_{f,H}/D_{f,N})} \quad (23)$$

$$K_H = -3 \times 10^{-5}(Q_R + Q)^2 + 0.580(Q_R + Q) + 13.6 \quad (24)$$

4.2. Assessment of the correction factors β_N and β_H for K_N and K_H

As was already mentioned in Section 2, K_N and K_H were found to vary slightly with different values of the average bulk concentration of the rate-limiting substrate (i.e. N_{av} or H_{av}). The assumption here is that the concentration of the rate-limiting substrate governs the following mechanisms: (1) deviation from intrinsic zero-order kinetic: at higher concentration of the rate-limiting substrate, higher fraction of the penetration depth is dominated by intrinsic zero-order kinetic and K_N and K_H are increased; (2) effect of pH changes on q_{max}: at higher concentration of the rate-limiting substrate, higher penetration is achieved with the resulting formation of sub-biofilm layers working at higher pH gradient along the penetration depth. The gradual increase in pH along the penetration depth results in an increase in the maximal specific degradation rate q_{max} in the range of pH applied (i.e.,~7–9.5) [7], and therefore an increase in K_N and K_H; (3) homogeneity of the biofilm: since the biofilm layer is not truly homogeneous, at higher concentrations of the rate-limiting substrate more regions in the reactor experience full substrate penetration and further increases in concentration should not lead to an increase in denitrification rate as predicted by the standard overall rate expression based on half-order kinetics (i.e. Eqs. (15) and (16)). This should reduce K_N and K_H with the increase in concentration.

In general, the effect of mechanisms (1) and (2) requires positive correction, while the effect of mechanism (3) requires negative correction for K_N and K_H. The empirical correction factors β_N and β_H in Eqs. (15′) and (16′) reflect the overall correction required to compensate for the effect of these 3 mechanisms on K_N and K_H, respectively.

Following the assumption above, a second set of experiments with NO_3^--N as the rate limiting factor was performed in order to assess the effect of different N_{av} concentrations on β_N values at constant total flow rate of 8450 mL/min. The results for β_N as a function of N_{av} are shown in Fig. 3.

Fig. 3 shows the overall effects of the three mechanisms mentioned above on β_N as a function of N_{av}. In general, β_N increased with higher N_{av} values for $N_{av} < 12$ mg/L. For $N_{av} < 5$ mg/L (i.e. below the reference concentration where β_N was set to be 1) it is assumed that mechanism 1 (i.e. deviation from zero-order kinetic) dominated the overall effects of the three mechanisms. For N_{av} in the range of 5–12 mg/L, the increase of β_N with higher N_{av} values may be related to the effect of mechanism 2 (i.e. pH changes). For $N_{av} > 12$ mg/L mechanism 3 dominated the overall effects of the three mechanisms and β_N decreased with increased N_{av} values.

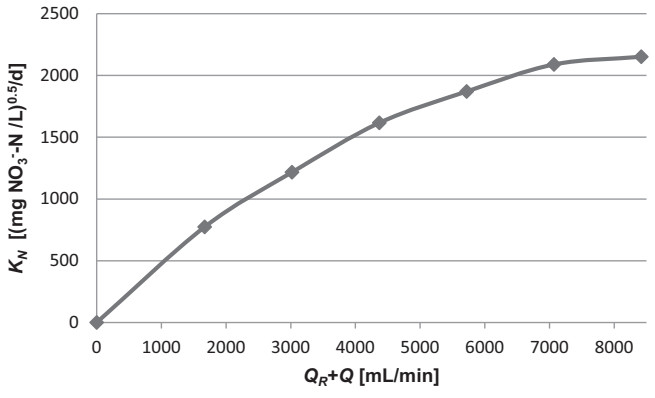

Fig. 2. K_N values at N_{av} = 5 mg NO_3^--N/L as a function of the total flow rate $Q_R + Q$.

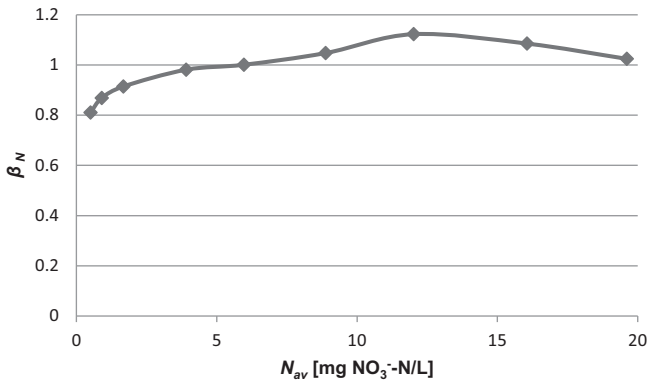

Fig. 3. The correction factor β_N for K_N as a function of different N_{av} concentrations at constant total flow rate ($Q_R + Q$) of 8450 mL/min.

A trend line for β_N with R-squared coefficient value of 0.9571 was derived from Fig. 3 (Eq. (25)).

$$\beta_N = -0.0017\ N_{av}^2 + 0.043\ N_{av} + 0.820 \quad (25)$$

A trend line for β_H (Eq. (26)) was derived by combining Eq. (25) and (21).

$$\beta_H = -0.0993\ H_{av}^2 + 0.334\ H_{av} + 0.821 \quad (26)$$

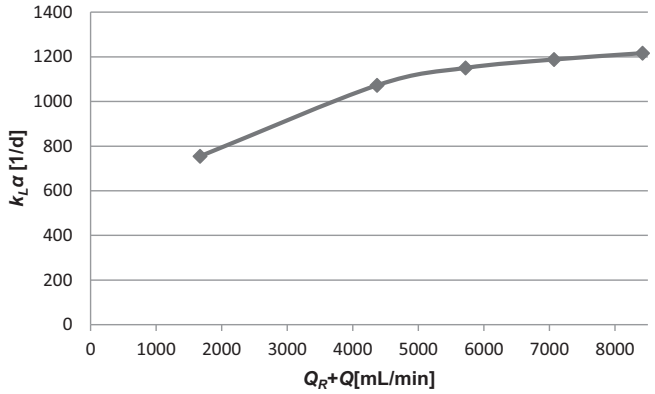

Fig. 4. The overall volumetric gas (H_2)-liquid mass transfer coefficient k_La as a function of the total flow rate $Q_R + Q$.

4.3. Assessment of k_La for different recirculation flow rates

Following the assessment of K_N, K_H, β_N and β_H, a third set of experiments was conducted in order to assess the overall volumetric gas (H_2)-liquid mass transfer coefficient k_La for different total flow rates. In this case, NO_3^--N was given in excess to ensure limitation of H_2. The results are shown in Fig. 4.

Fig. 4 shows that k_La values increased with higher recirculation flow rates. The main reason is the increase in media wetting for higher values of Q_R and therefore an increase in the gas-liquid interfacial surface area ($k_La = k_L\ x\ A/v$). Media wetting has been reported to be a prominent parameter affecting k_La in biotrickling filters for volatile organic compounds (VOCs) [18] and waste gases removal [19]. In both reports, k_La values for O_2 gas-liquid transfer in the range of 500–2500 1/d were reported. Estrada et al. also linked water recirculation intensity (expressed as liquid velocity) to k_La [20]. Reports on k_La values for other hydrogenotrophic denitrification systems were not found. A trend line for k_La with R-squared coefficient value of 0.9975 was derived (Eq. (27)).

$$k_L\alpha = -10^{-5}(Q_R + Q)^2 + 0.181(Q_R + Q) + 487 \quad (27)$$

The k_La value was not evaluated at lower recirculation flow rates which are not relevant for the operational conditions of the UFPR.

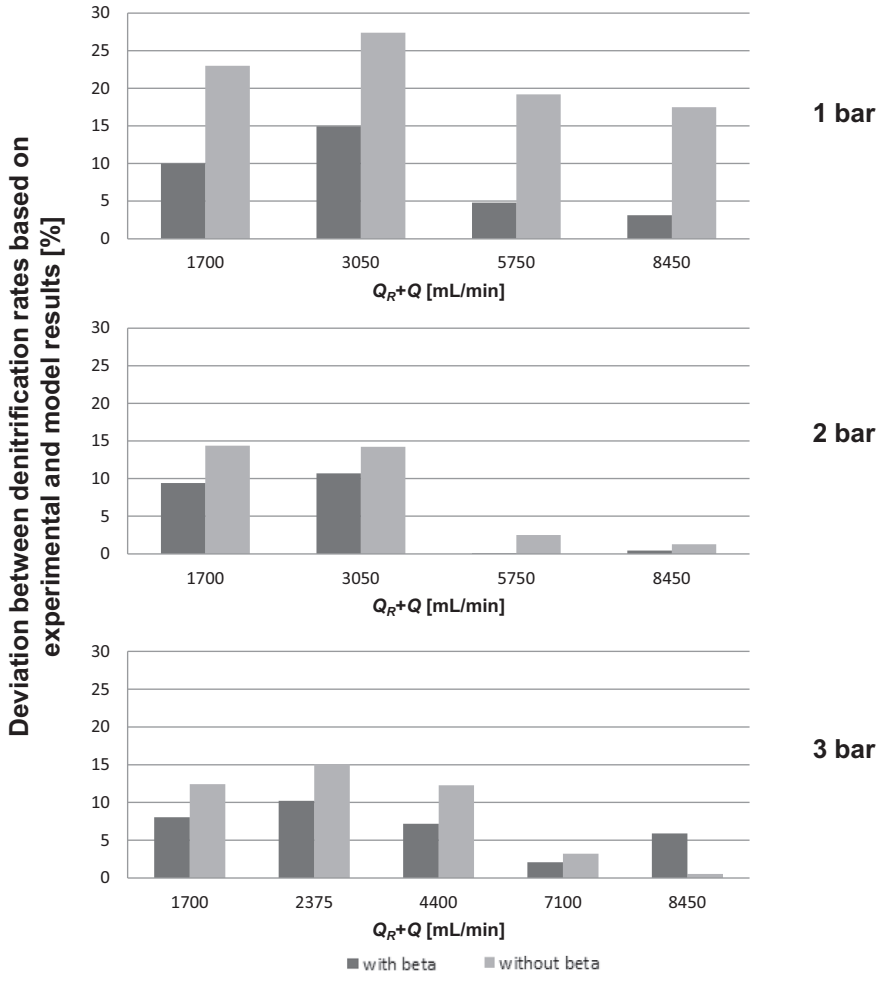

Fig. 5. Deviation between denitrification rates based on experimental and model results (*Y* axis) for different combinations of recirculation flow rate (*X* axis) and H_2 pressure – with and without the correction factor β (see legend).

4.4. Model validation

Following the evaluation of the intermediate variables (i.e. k_La, K_N, K_H, β_N and β_H), a set of experiments was conducted in order to validate the model. Denitrification rates measured for various combinations of recirculation flow rates (Q_R) and H_2 pressures were compared to those calculated by the model with and without the correction factor β. Normally, the UFPR is operated with closed headspace under a constant total pressure determined by the operator. During operation, the H_2 partial pressure decreases and is replaced by N_2 partial pressure (formed by denitrification) till a steady state is achieved with constant partial pressures of both gases. Here, however, the H_2 pressure in each of the experiments was maintained constant from the beginning by continuous flushing of the reactor's headspace with H_2 gas to ensure steady state conditions under a stable and known H_2 pressure within the reactor (the corresponding total pressure in normal operation will be higher than the H_2 pressure applied here). The deviation between model and experimental results for each of the combination is shown in Fig. 5.

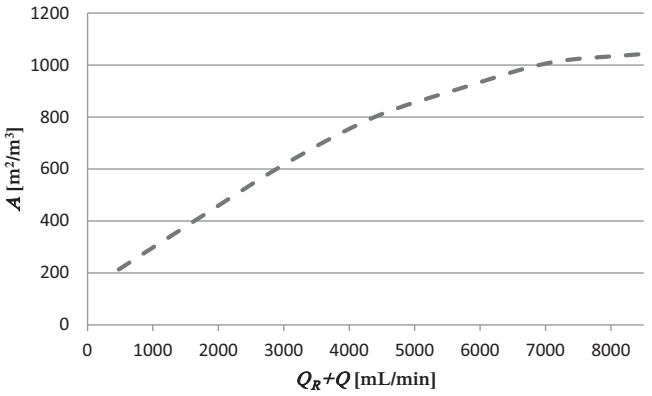

Fig. 6. Estimated active surface area A as a function of the overall loading rate $Q_R + Q$.

Fig. 5 shows clearly that the deviations between experimental and model results were lower with the correction factor β (except for the combination of Q_R = 8450 mL/min and H_2 pressure of 3 bars). By incorporating β, high correlation between experimental and model results was observed for all combinations of Q_R and H_2 pressure with average deviations of 8.2%, 5.2% and 6.7% for the trials with H_2 pressure of 1, 2 and 3 bars, respectively. These minor deviations corroborate the use of the model developed in the previous sections for further evaluation of the UFPR performance.

4.5. Performance Evaluation of the UFPR using the model

4.5.1. Evaluation of the active surface area A for different recirculation flow rates

The intrinsic maximal specific degradation rate of NO_3^--N $q_{max,N}$ and biofilm density X_f were found to be 0.606 g NO_3^--N/(gVSS·d) and 0.05 gVSS/mL, respectively, using the procedures described in Section 3. Following the estimation of $q_{max,N}$ and X_f, the maximal degradation rate of NO_3^--N within the biofilm $k_{0f,N}$ could be calculated by Eq. (2). Combining the calculated $k_{0f,N}$ value with K_N values calculated for the different total flow rates may be used for

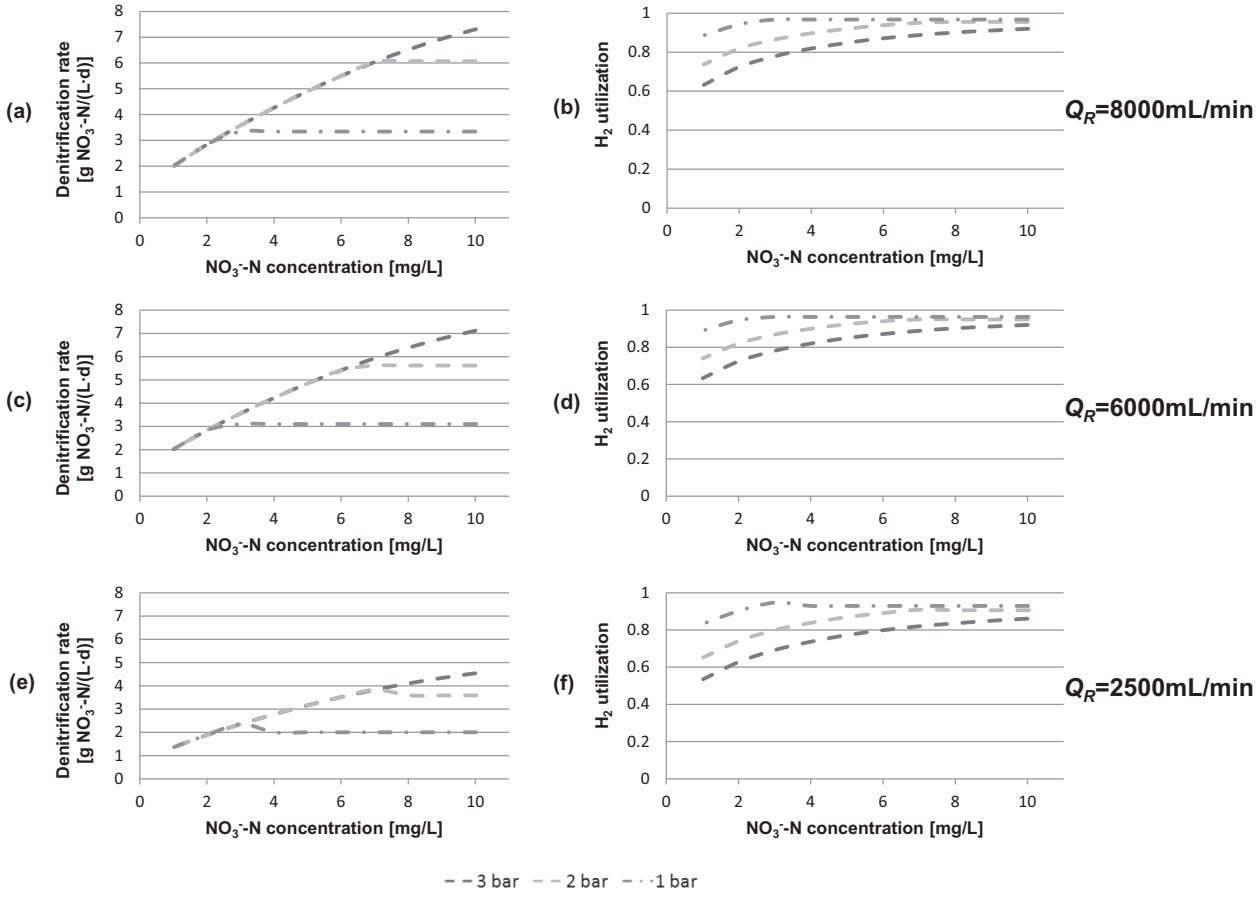

Fig. 7. Denitrification rate (a,c,e) and H_2 utilization efficiency (b,d,f) predicted by the model as a function of effluent NO_3^--N concentration for Q_R of 8000 mL/min (a,b), 6000 mL/min (c,d) and 2500 mL/min (e,f), and for H_2 pressure of 1, 2 and 3 bars (see legend below figures).

estimation of the active surface area A for different total flow rates ($K_N = A\sqrt{2D_{f,N}k_{0f,N}}$) by assuming constant average biofilm density (alternation of recirculation flow rates was performed for short periods and could hardly affect the average biofilm density). The results for the active surface area A calculated as a function of the total flow rate are shown in Fig. 6.

Fig. 6 shows that at the highest overall recirculation flow rate (i.e. $Q_R + Q = 8450$ mL/min), A is close to the value of the total surface area of the carriers provided by the manufacturer (i.e. 900 m^2/m^3). This fact correlates with the above assumption that a maximal media wetting is achieved at total flow rate of approximately 8450 mL/min. In general, it is possible that the maximal value for A estimated by the model is a bit higher than the one provided by the manufacturer due to biomass adherence to other surfaces within the reactor except for the carriers.

4.5.2. Evaluation of denitrification rate and H_2 utilization efficiency for different combinations of operational parameters

Denitrification rates and H_2 utilization efficiencies were evaluated by the model for various operational conditions (i.e. effluent NO_3^--N concentration, H_2 pressure and recirculation flow rate). The H_2 utilization efficiency was calculated by dividing H_2 consumption rate by the sum of H_2 consumption rate and H_2 loss through the effluent (Eq. (28)).

$$H_2\ utilization = r_H V/(r_H V + H_e Q) \quad (28)$$

Fig. 7 presents model results for denitrification rate (a,c,e) and H_2 utilization efficiency (b,d,f) as a function of the effluent NO_3^--N (N_e) for different combinations of Q_R and H_2 pressure (P_{H2}). Fig. 7 (a,c,e) shows that NO_3^--N limits denitrification rates at low NO_3^--N concentrations. At higher NO_3^--N concentrations, H_2 was found to be the rate-limiting substrate since no improvement in denitrification rate was observed with increasing the NO_3^--N concentration. In general, at higher H_2 pressure, higher denitrification rates can be achieved and the NO_3^--N concentration at which the transition to H_2 limitation occurs is also higher. The increase in recirculation flow rate Q_R has also a positive effect on denitrification rates as discussed in Section 4.1.

The H_2 utilization efficiency is positively affected by increasing Q_R, although only in a minor way (Fig. 7 (b,d,f)). The reason for this is the higher H_2 consumption rate in the biofilm due to better media wetting for higher Q_R [2]. Operation at higher NO_3^--N concentrations also improves H_2 utilization efficiency in the case of NO_3^--N limitation due to the higher demand for H_2 by the biofilm. Obviously, higher H_2 pressure has a negative effect on H_2 utilization efficiency. At higher H_2 pressure, a higher amount of unutilized H_2 gas is dissolved in the liquid phase and released with the effluent.

In general, higher denitrification rates together with higher utilization efficiencies of H_2 are achieved in the UFPR as compared to other hydrogenotrophic systems reviewed previously [2]. Fig. 7 shows that high denitrification rates of up to 7.5 g NO_3^--N/($L_{reactor}$·d) together with H_2 utilization efficiency above 90% can be attained by the UFPR for operation under the regulatory NO_3^--N concentrations of below 10 mg/L.

5. Conclusions

A mathematical model based on simple mass balances for steady-state and completely stirred hydraulic conditions was suggested for evaluating the performance of the novel unsaturated-flow pressurized reactor (UFPR) for hydrogenotrophic denitrification of groundwater. Increasing the total flow rate (i.e. recirculation + feed) up to 8450 mL/min with the corresponding recirculation ratio (Q_R/Q) of 18 had a positive influence on the active surface area available for biofilm growth and gas (H_2)-liquid mass transfer by improving media wetting. A correction factor β for the rate constant reduced the deviation between experimental and model results, by compensating for pH changes within the biofilm, deviation from intrinsic zero-order degradation kinetics and non-homogeneity of the biofilm. The addition of the correction factor resulted in a maximal deviation between measured and modeled denitrification rates of approximately 8%. Model results showed that high denitrification rates of up to 7.5 g NO_3^--N/($L_{reactor}$·d) together with H_2 utilization efficiency above 90% can be achieved in the UFPR. The principles for process evaluation using the model were described, making the treatment scheme proposed here easily adjustable to various regulatory requirements and water characteristics.

References

[1] K.A. Karanasios, I.A. Vasiliadou, S. Pavlou, D.V. Vayenas, Hydrogenotrophic denitrification of potable water: a review, J. Hazard. Mater. 180 (2010) 20–37, http://dx.doi.org/10.1016/j.jhazmat.2010.04.090.

[2] R. Epsztein, M. Beliavski, S. Tarre, M. Green, High-rate hydrogenotrophic denitrification in a pressurized reactor, Chem. Eng. J. 286 (2016) 578–584.

[3] E.H. Eding, A. Kamstra, J.A.J. Verreth, E.A. Huisman, A. Klapwijk, Design and operation of nitrifying trickling filters in recirculating aquaculture: a review, Aquacult. Eng. 34 (2006) 234–260, http://dx.doi.org/10.1016/j.aquaeng.2005.09.007.

[4] G.T. Daigger, J.P. Boltz, Trickling filter and trickling filter – suspended growth process design and operation: a state-of-the-art review, Water Environ. Res. 83 (2011) 388–404, http://dx.doi.org/10.2175/106143010X12681059117210.

[5] B.E. Logan, S.W. Hermanowicz, D.S. Parker, A fundamental model for trickling filter process design, J. Water Pollut. Control Fed. 59 (1987) 1029–1042.

[6] J.S. Devinny, J. Ramesh, A phenomenological review of biofilter models, Chem. Eng. J. 113 (2005) 187–196, http://dx.doi.org/10.1016/j.cej.2005.03.005.

[7] B. Rezania, N. Cicek, J.A. Oleszkiewicz, Kinetics of hydrogen-dependent denitrification under varying pH and temperature conditions, Biotechnol. Bioeng. 92 (2005) 900–906, http://dx.doi.org/10.1002/bit.20664.

[8] C.X. Lu, P. Gu, Hydrogenotrophic denitrification for the removal of nitrate in drinking water, Huanjing Kexue/Environ. Sci. 29 (2008) 671–676.

[9] S. Ghafari, M. Hasan, M.K. Aroua, A kinetic study of autohydrogenotrophic denitrification at the optimum pH and sodium bicarbonate dose, Bioresour. Technol. 101 (2010) 2236–2242, http://dx.doi.org/10.1016/j.biortech.2009.11.068.

[10] B. Atkinson, I.J. Davies, The overall rate of substrate uptake (reaction) by microbial films: part 1, a biological rate equation, Trans. Inst. Chem. Eng. 52 (1974) 248–259.

[11] P. Harremoes, Biofilm kinetics, Water Pollut. Microbiol. 2 (1978) 71–109.

[12] W.G. Whitman, The two-film theory of gas absorption, Chem. Metall. Eng. 29 (1923) 146–148.

[13] B.E. Logan, Oxygen transfer in trickling filters, J. Environ. Eng. 119 (1994) 1059–1076.

[14] M. Boller, W. Gujer, Nitrification in tertiary trickling filters followed by deep-bed filters, Water Res. 20 (1986) 1363–1373.

[15] P.L. McCarty, Stoichiometry of biological reactions, Proc. Int. Conf. Towar. A Unified Concept Biol. Waste Treat. Des., Atlanta, Georgia, 1972.

[16] C. Glass, J. Silverstein, Denitrification kinetics of high nitrate concentration water: pH effect on inhibition and nitrite accumulation, Water Res. 32 (1998) 831–839, http://dx.doi.org/10.1016/S0043-1354(97)00260-1.

[17] P.S. Stewart, Diffusion in biofilms, J. Bacteriol. 185 (2003) 1485–1491.

[18] P.S. Valero, C. Gabaldon, J.P. Roja, M.C. Perez, Study of mass oxygen transfer in a biotrickling filter for air pollution control, Procedia Eng. 42 (2012) 1726–1730.

[19] A.R. Pedersen, E. Arvin, Removal of toluene in waste gases using a biological trickling filter, Biodegradation 6 (1995) 109–118.

[20] J.M. Estrada, A. Dudek, R. Munoz, G. Quijano, Fundamental study on gas-liquid mass transfer in biotrickling filter packed with polyurethane foam, J. Chem. Technol. Biotechnol. 89 (2013) 1419–1424.